Novel 4-Oxo-1,4-dihydroquinoline-3-carboxamide Derivatives as New CB_2 Cannabinoid Receptors Agonists: Synthesis, Pharmacological Properties and Molecular Modeling

Eric Stern,[†,‡] Giulio G. Muccioli,[†,§] Régis Millet,[‡] Jean-François Goossens,[‡] Amaury Farce,[||] Philippe Chavatte,[||] Jacques H. Poupaert,[§] Didier M. Lambert,[§] Patrick Depreux,*[,‡] and Jean-Pierre Hénichart[‡]

Institut de Chimie Pharmaceutique Albert Lespagnol, Université de Lille 2, EA 2692, 3 rue du Pr. Laguesse, B.P. 83, F-59006 Lille, France, Unité de Chimie pharmaceutique et de Radiopharmacie, Ecole de Pharmacie, Faculté de Médecine, Université catholique de Louvain, 73 avenue E. Mounier UCL-CMFA (7340), B-1200 Bruxelles, Belgium, and Faculté de Pharmacie, Laboratoire de Chimie Thérapeutique, Université de Lille 2, EA 1043, 3 rue du Professeur Laguesse, B.P. 83, F-59006 Lille, France

Received May 18, 2005

Recent data indicated that the CB_2 cannabinoid receptor constitutes an attractive drug target due to its potential functional role in several physiological and pathological processes. A set of 4-oxo-1,4-dihydroquinoline-3-carboxamide derivatives, characterized by the presence of some important structural requirements exhibited by other classes of cannabinoid ligands, such as an aliphatic or aromatic carboxamide group in position 3, and an alkyl or benzyl group in position 1, was synthesized and assayed to measure their respective affinity for both human CB_1 and CB_2 cannabinoid receptors. The results indicate that these 3-carboxamido-quinolones derivatives exhibited a CB_2 receptor selectivity, particularly derivatives **28**−**30**, and **32*R***. Moreover, in the [^{35}S]-GTPγS binding assay, all the compounds behaved as CB_2 receptor agonists. Molecular modeling studies showed that compound **30** interacts with the CB_2 receptor through a combination of hydrogen bond and aromatic/hydrophobic interactions. In conclusion, 4-oxo-1,4-dihydroquinoline-3-carboxamide derivatives constitute a new class of potent and selective CB_2 cannabinoid receptors agonists.

Introduction

Hashish and marijuana, two preparations derived from the Indian hemp *Cannabis Sativa L.*, have been used since immemorial time for their medicinal and psychoactive properties. Despite the isolation of Δ^9-tetrahydrocannabinol (Δ^9-THC, Chart 1) as the major psychoactive component of *Cannabis Sativa L.*[1] in the 1960s, the molecular targets of Δ^9-THC were only discovered in the late 1980s, with on one hand the help of a synthetic radioligand [^{3}H]-CP-55,940 [2] (Chart 1) allowing suitable cannabinoid receptor binding assays and, on the other hand, the characterization of the biochemistry and the molecular biology of cannabinoid receptors, which led to two subtypes of G-protein coupled receptors named CB_1[3] and CB_2[4] cannabinoid receptors. They differ in sequences, tissue localization, and, to some extent, signal transduction mechanisms. In addition, generation of knock-out mice models where either one subtype or two subtypes genes have been deleted suggest the putative existence of additional cannabinoid receptors.[5]

The cannabinoid CB_1 receptor is nowadays extensively studied due to its implication both in the therapeutic and psychoactive effects of cannabinoids in the central nervous system. Transduction mechanisms of cannabinoid CB_1 receptors involve inhibition of cAMP production through inhibition of adenylate cyclase,[6] inhibition of calcium influx,[7,8] activation of potassium channels,[9] and activation of the MAP kinase pathway.[10]

Promising selective cannabinoid CB_1 receptor antagonists such as rimonabant or SLV-319 are currently under investigation in clinical human studies for the treatment of obesity and the associated metabolic syndrome.[11] On the contrary, Δ^9-THC and nabilone are currently marketed to reduce emesis and/or prevent cachexia in AIDS or cancer patients.[12] Other therapeutic applications currently studied include multiple sclerosis, neuropathic, and cancer pain.

Despite the discovery by sequence homology of the CB_2 cannabinoid receptor in the same years, the physiological as well as putative therapeutic potential of this receptor largely remains unexplored. However, recent data indicate that CB_2 cannabinoid receptors participate in the control of peripheral pain,[13,14] inflammation,[15] and cancer proliferation.[16] It also has an antifibrogenic role in the liver.[17] Moreover, the recent discovery of the presence of the CB_2 cannabinoid receptors in the brain microglial cells[18,19] gave a rationale for prevention of Alzheimer's disease pathology by cannabinoid agents. Indeed, it was recently shown that CB_2 cannabinoid receptor agonists might provide neuroprotection by blockade of microglial activation.[20]

Both types of cannabinoid receptors are sensitive to pertussis toxin, suggesting their predominant coupling to G_i-type proteins allowing the use of [^{35}S]-GTPγS assay[21] to characterize the functionality of cannabinoid ligands. Cannabinoid receptors are activated by endocannabinoids, long-chain polyunsaturated fatty acids where the carboxylate group is either amidated by ethanolamine or esterified by glycerol.[22] The two major representatives are anandamide (*N*-arachidonylethanolamine) and 2-AG (2-arachidonoylglycerol) (Chart 1), respectively.

On a pharmacological point of view, up to now, the cannabinoid ligands might be divided into three major categories: (a) compounds which are not, or poorly, selective for one cannabinoid receptor subtype such as classical cannabinoids (Δ^9-THC and related compounds), nonclassical cannabinoids (e.g., CP-55,940 and derivatives), and aminoalkylindoles (e.g., WIN-55,212-2); (b) compounds which are selective for the cannabinoid CB_1 receptor subtype such as some biarylpyrazoles (e.g., SR-141716A) and many other diverse heterocyclic structures

[†] Both authors contributed equally to this work.

[‡] Institut de Chimie Pharmaceutique Albert Lespagnol, Université de Lille 2.

[§] Université Catholique de Louvain.

[||] Faculté de Pharmacie, Université de Lille 2.

* To whom correspondence should be addressed. Phone: +33-3-2096-4379. Fax: +33-3-2096-4906. E-mail: pdepreux@pharma.univ-lille2.fr.

10.1021/jm050467q CCC: $33.50
Published on Web 12/13/2005

Chart 1. Representative Ligands of the Cannabinoid Receptors

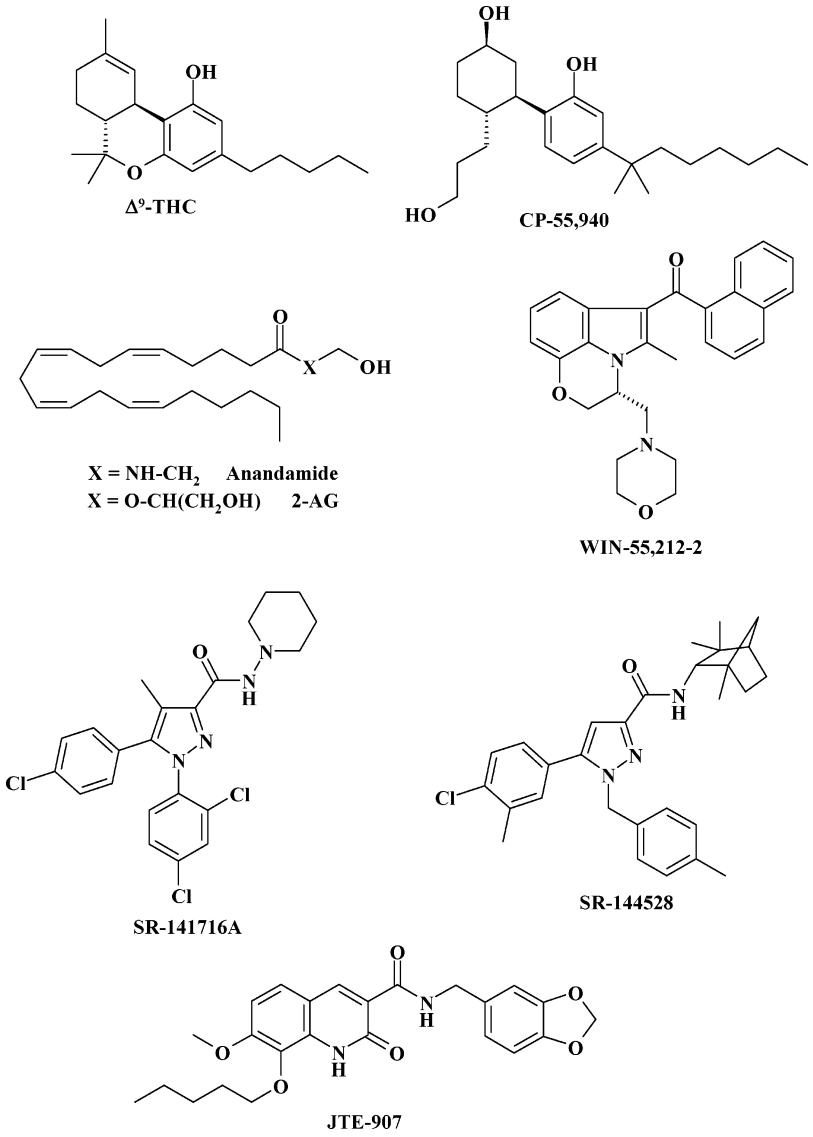

such as triazoles,[23] thiazoles,[24] imidazoles,[24,25] imidazolidinediones,[26] 2-thioxoimidazolidinones,[27] and pyridines[28] that have been recently reported; and (c) a few compounds that are selective for the CB_2 cannabinoid receptor subtype such as some biarylpyrazoles (e.g., SR-144528), 1,2-dihydroquinoline-3-carboxamide (JTE-907, Chart 1),[29] 1,8-naphthyridines,[30] and triaryl bis-sulfones.[31]

At present, new potent CB_2-selective cannabinoid receptor ligands are important to understand some of the physiological effects of cannabinoids, such as their immunosuppressive, anti-inflammatory, and antinociceptive activities.[32−37] For instance, it was very recently shown that low doses of Δ^9-THC could reduce atherosclerosis in mice by acting at the CB_2 cannabinoid receptor.[38] Finally but not least, cannabinoid agonists that selectively target CB_2 cannabinoid receptors should be devoid of psychoactive effects.

Along this line, the present paper describes the synthesis and the pharmacological properties of a set of 27 4-oxo-1,4-dihydroquinoline-3-carboxamide derivatives, with various substitutions on the heterocyclic nucleus, as illustrated in Chart 2.

Aliphatic or aromatic carboxamide groups in position 3 have been selected on the basis of other cannabinoid pharmacophores—such as those present both in the quinolone derivative JTE-907 and in the biarylpyrazole SR-144528—and a hydrophobic

Chart 2. General Structure of 4-Oxo-1,4-dihydroquinoline-3-carboxamide Derivatives **11**−**36**

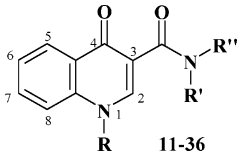

substituent in position 1 as in the aminolakylindole derivatives.[39] They were tested in competitive binding assays toward both human CB_1 ($h$$CB_1$) and CB_2 ($h$$CB_2$) cannabinoid receptors expressed in CHO cells[40] and were found selective for the CB_2 cannabinoid receptor subtype. For compounds exhibiting a K_i value lower than 1 μM, [^{35}S]-GTPγS binding assays were performed to determine their functionality.[32] Additionally, overlay of WIN-55,212-2, CP-55,940, and **30** allowed us to study their structural similarities. Docking was finally performed to elucidate the mode of interaction of compound **30** with a CB_2 cannabinoid receptor model.

Results

Chemistry. The synthetic routes to obtain the target 4-oxo-1,4-dihydroquinoline-3-carboxamide derivatives **11**−**36** are outlined in Scheme 1. All substituents are summarized in Table

Scheme 1. Synthesis of the 4-Oxo-1,4-dihydroquinoline-3-carboxamide Derivatives 11−36[a]

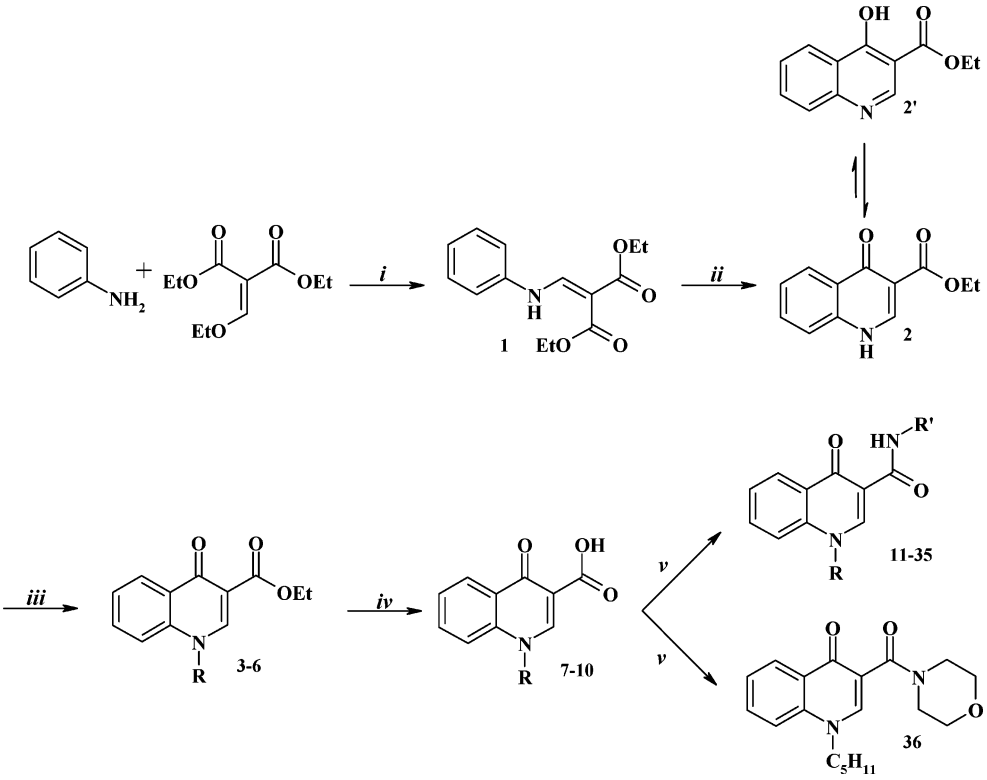

[a] Reagents and conditions: (*i*), 100 °C, 91%; (*ii*) Ph−O−Ph, reflux, 77%; (*iii*) R−X, NaH, DMF, 90 °C, 50−93%; (*iv*) NaOH, EtOH, 100 °C, 70−76%; (*v*) R′−NH_2 or morpholine, PyBRoP, PS−HOBt (HL), DIEA, DMF, rt, 14−97%.

1. Compounds **11**−**36** were obtained by a coupling reaction between selected amines and 4-oxo-1,4-dihydroquinoline-3-carboxylic acids **7**−**10** obtained in three steps following Gould−Jacobs' procedure.[41,42]

To afford the 4-oxo-1,4-dihydroquinoline-3-carboxylic acid ethyl ester **2**, extreme conditions (i.e., reflux of **1** at ∼ 255°C in diphenyl ether[43]) were required to induce cyclization. In this process, as observed by ^{1}H NMR, the 4-quinolone form **2**, and not its 4-hydroxy-quinoline tautomeric form **2′**, was obtained. *N*-alkylation of **2** in anhydrous DMF with appropriate alkyl bromides or benzylbromide in the presence of sodium hydride gave the 1-alkyl-4-oxo-1,4-dihydroquinoline-3-carboxylic acid ethyl esters **3**−**6**.[44] Hydrolysis in 10% aqueous NaOH yielded the corresponding 1-alkyl-4-oxo-1,4-dihydroquinoline-3-carboxylic acids **7**−**10**.[45]

To obtain some chemical diversity among 1-alkyl-4-oxo-1,4-dihydroquinoline-3-carboxamides, a solid phase procedure was set up using a previously reported polystyrene-supported HOBt as coupling reagent.[46,47] The reaction performed on a Quest 205 synthesizer according to the general reaction pathway outlined in Scheme 2 generated compounds **11**−**36**. This is a two-step procedure: (i) formation of the polymer bound activated ester of the carboxylic acid (**7**−**10**) using bromotrispyrrolidinophosphonium hexafluorophosphate (PyBrop); (ii) release of the target amide in solution by addition of the amine. Optimization of both steps was performed to obtain a solution of amide free of byproducts. The best conditions for activation were found to be 2 × 3 h activating time step in DMF. The coupling step was achieved in 24 h with 0.9 equiv of the amine in a DMF solution. The target compounds **11**−**36** were purified either by recrystallization or by preparative thick-layer chromatography. The *N*(1) alkylation was confirmed by 2D ^{1}H NMR (ROESY) as evidenced by the presence of cross-peaks between H(2) and N−CH_2 protons.

Table 1. Structures and Percentages of Displacement of [^{3}H]-SR-141716A and [^{3}H]-CP-55,940, Respectively, by Compounds **8**−**36** (10 μM) on *h*CB_1 and *h*CB_2 Cannabinoid Receptors[a]

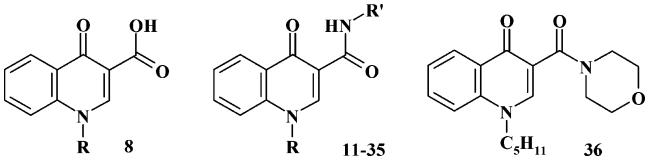

compd	R′	R	% of displacement CB_1−R	% of displacement CB_2−R
8		*n*-pentyl	<20	<15
11	4-methoxyphenyl	*n*-butyl	<20	50.5 ± 6.9
12	4-methoxyphenyl	*n*-pentyl	<20	60.1 ± 7.6
13	4-methoxyphenyl	*n*-hexyl	<10	28.2 ± 8.0
14	1-naphthyl	*n*-butyl	45.3 ±.7.4	85.4 ± 6.3
15	1-naphthyl	*n*-pentyl	65.9 ± 6.8	90.6 ± 1.3
16	1-naphthyl	*n*-hexyl	53.3 ± 7.4	80.0 ± 6.6
17	benzyl	*n*-butyl	33.6 ± 6.5	44.9 ± 6.7
18	benzyl	*n*-pentyl	50.5 ± 5.5	66.7 ± 8.1
19	benzyl	*n*-hexyl	37.4 ± 4.0	54.6 ± 6.5
20	4-methoxybenzyl	*n*-pentyl	<10	51.7 ± 4.3
21	2-naphthyl	*n*-pentyl	<10	63.9 ± 4.1
22	2-phenylethyl	*n*-pentyl	64.8 ± 5.1	98.2 ± 2.9
23	3-phenylpropyl	*n*-pentyl	32.8 ± 4.8	85.5 ± 6.0
24	3,4-dichlorophenyl	*n*-pentyl	<10	68.1 ± 3.0
25	4-cyanophenyl	*n*-pentyl	49.6 ± 3.3	79.4 ± 6.0
26	4-biphenyl	*n*-pentyl	<20	<20
27	2-(benzo[1,3]dioxol-5-yl)ethyl	*n*-pentyl	43.6 ± 2.0	88.7 ± 1.7
28	1-adamantyl	*n*-pentyl	59.0 ± 3.9	104.0 ± 3.9
29	2-adamantyl	*n*-pentyl	37.8 ± 3.3	103.8 ± 1.8
30	1-(3,5-dimethyl)adamantyl	*n*-pentyl	54.6 ± 2.4	95.6 ± 5.4
31	1-(3,5-dimethyl)adamantyl	benzyl	32.5 ± 1.4	86.3 ± 2.1
32	(*RS*)-1-phenylethyl	*n*-pentyl	68.3 ± 3.1	101.1 ± 3.2
33	(*RS*)-1-(2-naphthyl)ethyl	*n*-pentyl	<10	82.9 ± 3.7
34	(*RS*)-1-(1-naphthyl)ethyl	*n*-pentyl	35.5 ± 3.7	98.9 ± 4.1
35	(*RS*)-1-(1,2,3,4-tetrahydro-naphthyl)	*n*-pentyl	79.7 ± 4.1	96.5 ± 4.0
36		*n*-pentyl	<10	36.5 ± 3.4

[a] Mean ± SEM of at least four experiments performed in duplicate.

Scheme 2. Solid-Phases Procedure of the Synthesis of the 4-Oxo-1,4-dihydroquinoline-3-carboxamide Derivatives 11−36[a]

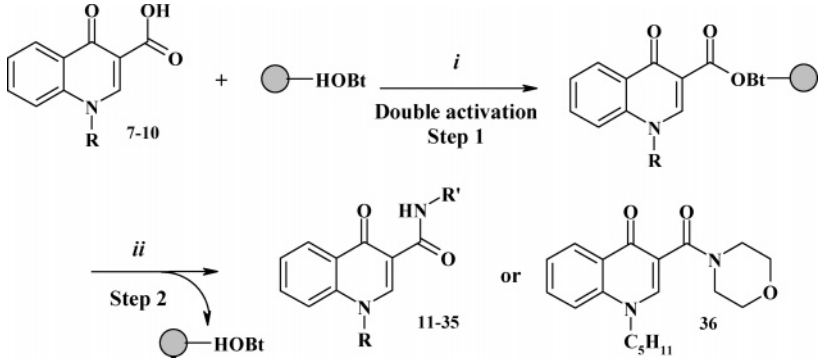

[a] Reagents and conditions: (*i*) PyBRoP, PS−HOBt (HL), DIEA, DMF, rt; (*ii*) R′−NH_2 or morpholine, DMF, rt.

Table 2. Affinities of Selected Derivatives and of Reference Compounds (SR-144528, WIN-55,212-2, CP-55,940, JWH-133, and HU-210) at the *h*CB_2 Cannabinoid Receptor[a]

compd	*h*CB_2 cannabinoid receptor K_i (nM)
14	455 ± 63
15	371 ± 34
16	844 ± 78
18	>1000
22	201 ± 28
23	>1000
24	>1000
25	772 ± 72
27	426 ± 39
28	16.4 ± 1.5
29	13.4 ± 1.2
30	15.8 ± 1.4
31	664 ± 62
32	70.8 ± 9.1
32*R*	37.1 ± 3.4
32*S*	784 ± 71
33	>1000
33*R*	584 ± 54
33*S*	>5000
34	174 ± 16
34*R*	125 ± 12
34*S*	>1000
35	60.2 ± 5.5
SR-144528	51.7 ± 4.8
WIN-55,212-2	9.1 ± 0.8
CP-55,940	15.4 ± 1.4
JWH-133	20.3 ± 2.6
HU-210	7.3 ± 0.9

[a] The K_i values were obtained from nonlinear analysis of competition curves using [^{3}H]-CP-55,940 as radioligand. Data are the mean ± SEM of at least four experiments performed in duplicate.

Pharmacology. The 4-oxo-1,4-dihydroquinoline-3-carboxamide derivatives (**11**−**36**) were screened at 10 μM concentrations for their affinity and selectivity toward the *h*CB_1 and *h*CB_2 cannabinoid receptors in a competitive binding experiment as previously described.[48] Membranes from Chinese hamster ovarian (CHO) cells expressing either the *h*CB_1 or the *h*CB_2 cannabinoid receptors were used in these experiments. [^{3}H]-SR-141716A and [^{3}H]-CP-55,940 at concentrations of 1 nM were used as radioligands for the *h*CB_1 and the *h*CB_2 cannabinoid receptor, respectively. The results expressed as the displacement percentages of the radioligand from its binding site are summarized in Table 1. The K_i values were then determined for compounds exhibiting a specific displacement superior to 60% either for the cannabinoid *h*CB_2 (Table 2) or the *h*CB_1 receptors (Table 3). The selectivity ratio is presented in the Table 3 when K_i values have been obtained for both receptors. All together these results indicated that the 4-oxo-1,4-dihydroquinoline-3-carboxamide derivatives (**11**−**36**) are selective for the CB_2 cannabinoid receptors.

Table 3. Affinities of Selected Derivatives (Compounds **15**, **29**, **32*R***, and **35**) and of Reference Cannabinoid (SR-141716A) at the *h*CB_1 Cannabinoid Receptor[a]

compd	*h*CB_1 cannabinoid receptor K_i (nM)	selectivity ratio CB_2 versus CB_1
15	4083 ± 375	11
29	1925 ± 179	143
32*R*	1154 ± 108	31
35	1045 ± 96	17
SR-141716A	5.37 ± 0.6	

[a] The K_i values were obtained from nonlinear analysis of competition curves using [^{3}H]-SR-141716A as radioligand. Data are the mean ± SEM of at least four experiments performed in duplicate.

The question of the 4-oxo-1,4-dihydroquinoline-3-carboxamide derivatives functionality was investigated by using a [^{35}S]-GTPγS binding assay.[49] This assay constitutes a functional measure of the interaction of the receptor and the G-protein, the first step in activation of the G-protein coupled receptors. It is a useful tool to distinguish between agonists (increasing the nucleotide binding), inverse agonists (decreasing the nucleotide binding), and neutral antagonists (not affecting the nucleotide binding). The reference cannabinoid agonists JWH-133, HU-210, WIN-55,212-2, and CP-55,940 as well as the inverse agonist SR-144528 were assayed in a [^{35}S]-GTPγS binding stimulation assay at the *h*CB_2 cannabinoid receptors. Results expressed as percentages of the basal stimulation (set at 100%) are summarized in Table 4. In this model, agonists at 10 μM give a [^{35}S]-GTPγS binding stimulation from 128 to 149% of basal stimulation, while the inverse agonist SR-144528 abolishes it to 22%. 4-Oxo-1,4-dihydroquinoline-3-carboxamide derivatives **14**−**16**, **18**, **22**−**25**, and **27**−**35** were challenged in this assay and gave values from 117 up to 137% of basal stimulation indicating that these compounds act as agonists at the *h*CB_2 cannabinoid receptors. To further investigate the agonistic properties, the potency and efficacy of compounds **29**, **30**, **32*R***, and **35** were determined (Table 5). These compounds dose-dependently increased the [^{35}S]-GTPγS binding, exhibiting EC_{50} values of the same magnitude as the respective K_i values. For instance, compounds **30** and **32*R*** exhibited EC_{50} values of 14.1 and 16.8 nM, respectively.

Structure−Affinity Relationships. Preliminary screening results showed that the first 3-carboxamidoquinolone derivatives studied displayed affinity for the cannabinoid receptors and therefore could constitute a suitable template in the design of new cannabinoid derivatives. In addition, a selectivity profile for the *h*CB_2 subtype was observed. To define the correct profile for binding to the *h*CB_2 cannabinoid receptor, we decided to

Table 4. [^{35}S]-GTPγS Binding Stimulation Assays (10 μM) of Selected Compounds and Reference Cannabinoid Ligands (SR-144528, WIN-55,212-2, CP-55,940, JWH-133, and HU-210) for the *h*CB_2 Cannabinoid Receptors[a]

compd	*h*CB_2 cannabinoid receptor [^{35}S]-GTPγS specific binding (% of basal)
14	131.8 ± 3.5**
15	123.7 ± 3.8**
16	123.9 ± 2.4**
18	128.6 ± 2.3**
22	135.7 ± 2.5**
23	133.7 ± 2.2**
24	116.5 ± 0.8**
25	133.1 ± 1.1**
27	136.5 ± 1.3**
28	125.6 ± 2.5**
29	129.6 ± 1.1**
30	130.7 ± 1.8**
31	121.0 ± 2.0**
32	130.5 ± 1.0**
32*R*	123.6 ± 1.4**
33	122.5 ± 1.7**
33*R*	122.3 ± 2.1**
34	116.8 ± 1.0**
34*R*	119.2 ± 0.8**
35	123.1 ± 1.1**
SR-144528	21.6 ± 2.7**
WIN-55,212-2	127.8 ± 2.3**
CP-55,940	145.6 ± 1.8**
JWH-133	148.0 ± 2.5**
HU-210	135.0 ± 1.4**

[a] Results are expressed as the percentages of stimulation of [^{35}S]-GTPγS binding (basal value set at 100%). Data are the mean ± SEM of three experiments performed in duplicate. Statistical significance was assessed by one-way ANOVA followed by a Dunett post-test (*P < 0.05 and **P < 0.01).

Table 5. Determination of the Potency and Efficacy of Compounds **29**, **30**, **32*R***, **35**, SR-144528, WIN-55,212-2, CP-55,940, JWH-133, and HU-210 at the *h*CB_2 Cannabinoid Receptors

compd	EC_{50} (nM)	E_{max} (%)
29	24.8 ± 3.4	126.0 ± 1.0
30	14.1 ± 5.6	124.1 ± 0.8
32*R*	16.8 ± 4.1	128.7 ± 1.2
35	157.4 ± 54	123.5 ± 1.5
SR-144528	2.1 ± 1.1	21.6 ± 2.7
WIN-55,212-2	24.6 ± 1.7	126.2 ± 1.5
CP-55,940	6.1 ± 2.1	145.6 ± 2.98
JWH-133	145.6 ± 3.0	149.0 ± 3.2
HU-210	4.1 ± 1.3	135.1 ± 3.4

[a] E_{max} results are expressed as the percentages of stimulation of [^{35}S]-GTPγS binding (basal value set at 100%). Data are the mean ± SEM of three experiments performed in duplicate. The EC_{50} values were obtained from nonlinear analysis of [^{35}S]-GTPγS binding curves. Data are the mean ± SEM of at least three experiments performed in duplicate.

investigate structure modifications on quinolone nucleus either by introducing various alkyl side chains on the N_1 nitrogen or by varying the substitution of the amide nitrogen.

A first set of nine compounds was synthesized (**11**−**19**). These compounds encompassed an N_1-alkyl side chain (butyl, pentyl or hexyl) and a 4-methoxyphenyl, 1-naphthyl, or benzyl carboxamido substituent. In these series, the 1-naphthyl derivatives showed the highest affinity and, regardless of the nature of the carboxamido substituent, the *n*-pentyl group proved to be more potent than the *n*-butyl or *n*-hexyl. The highest *h*CB_2 cannabinoid receptor affinity was found for compound **15** (K_i = 371 nM). Therefore, to continue our investigation, we decided to keep the *n*-pentyl residue constant and develop a library of compounds with various 3-carboxamido substituents.

The *h*CB_2 receptor binding data (Table 2) revealed that the affinity is quite sensitive to the 3-carboxamido group modifications. Indeed, replacement of 1-naphthyl (**15**) by the 2-naphthyl isomer (**21**) resulted in a decreased affinity. However, replacement of the benzyl group (**18**) by 4-methoxybenzyl (**20**) and replacement of the 4-methoxyphenyl group (**12**) by 4-cyanophenyl (**25**) or 3,4-dichlorophenyl (**24**) did not elicit a clear effect on affinity. Therefore, electronic effects on the aromatic moiety did not influence the affinity for the cannabinoid CB_2 receptor.

We also synthesized 2-phenylethyl (**22**), 3-phenylpropyl (**23**), 4-biphenyl (**26**), and 2-(benzo[1,3]dioxol-5yl)ethyl (**27**) derivatives in order to evaluate the importance of hydrophobic character in the 3-position, since 1-naphthyl (**15**) revealed a good affinity for CB_2 receptor (K_i = 371 nM). The best result was found with **22** (K_i = 204 nM) when the phenyl group was spaced from the 3-carboxamidoquinolone ring by an ethyl link. Replacement of this ethyl link by methyl or propyl homologues led to a decreased affinity (K_i values > 1000 nM) that was even more markedly observed in the 4-biphenyl derivative (**26**, <20% displacement at 10 μM). Compound **27**, in which the phenethyl substituent of **22** is replaced by a 2-(benzo[1,3]dioxol-5yl)ethyl, showed about 2-fold less affinity (K_i = 426 nM).

Nonaromatic compounds with different adamantyl substituents (**28**, **29**, **30**, **31**) were also investigated. These moieties are widely found in the structure of cannabinoid ligands[11,50] with antagonistic properties. They can also generate hydrophobic interactions. These modifications induced a marked improvement in affinity (K_i values of 16.4 nM and 13.4 nM for **28** and **29**, respectively). Interestingly, in the [^{35}S]-GTPγS binding assay, these compounds kept their agonistic properties. Enhancement of adamantyl hydrophobicity by addition of two methyl groups (in position 3 and 5) did not elicit a marked effect on affinity as shown by compound **30** (K_i = 15.8 nM). Compound **31** in which the *n*-pentyl side chain is replaced by a benzyl showed about 44-fold less affinity (K_i = 664 nM). Replacement of the adamantyl substituent by a morpholino group, yielding compound **36**, resulted in a decreased affinity.

The cannabinoid *h*CB_2 receptor binding data reported herein suggested that the hydrophobicity of the carboxamido substituent appears to be as important as the aromatic character. In addition, the poor affinity of the 3-carboxylic acid intermediate **8** (<15% displacement at 10 μM) underlines the importance of the amide substitution. The carboxamido group is most likely located in a large hydrophobic cluster. To study the pocket, for the aromatic carboxamide compounds, a steric constraint by modulation of **22** using its 1-phenylethyl isomer (**32**) was introduced. The steric constraint imposed by a methyl group on the methylene spacer induced a particular orientation of the aromatic group. In this series, we also replaced the phenyl moiety by other aromatic nuclei: 1- and 2-naphthyl (**33** and **34**). Compounds **32**−**34** were first tested as racemates, as shown in Table 2. Introduction of this pseudo-rigidification led to an increase of the *h*CB_2 cannabinoid receptor affinity as illustrated by compounds **32** and **18** (K_i values of 70.8 and >1000 nM, respectively). Modification of the aromatic group, in compounds **33** (K_i > 1000 nM) and **34** (K_i = 174 nM), resulted in a decreased affinity. Compound **35**, corresponding to a constrained analogue of **32**, showed an affinity of the same magnitude (K_i values of 60.2 nM and 70.8 nM for **35** and **32**, respectively).

The enantiopure forms of **32**−**34**, respectively noted **32**−**34*R*** and **32**−**34*S***, synthesized starting from the corresponding enantiopure amine were also tested, as summarized in Table 2. In all cases, the *R* enantiomers exhibited about 10-fold higher affinity than the *S* enantiomers. The highest affinity was found in the eutomer **32*R*** (K_i = 37.1 nM). The distomer **32*S*** with an affinity of 776 nM highlighted that this chiral ligand binds

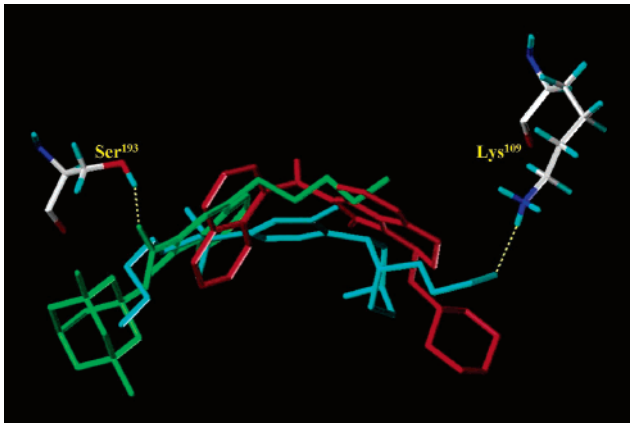

Figure 1. Receptor-based alignment results of WIN-55,212-2 (red), CP-55,940 (cyan), and **30** (green).

stereoselectively to the *h*CB_2 receptor. Introduction of this pseudo-rigidification induced an improvement of affinity for both of the two receptor subtypes.

Superposition and Docking Studies. Bovine rhodopsin was used for homology modeling of the CB_2 cannabinoid receptor as it is the only currently solved G-protein coupled receptor tridimensional structure. However, its crystallographic structure has been determined in a dark-adapted conformation which is probably an inactive form. Therefore, besides pure homology modeling, a more elaborated construction of the CB_2 cannabinoid receptor was required to approach its putative active conformation. Previous works performed on the CB_1 cannabinoid receptor have shown that transmembrane domains 3 and 6 (TM 3 and TM 6) should undergo a rotation around their axis to render the effect of an agonist binding.[51] We followed these conclusions to build a model of CB_2 cannabinoid receptor able to bind the 3-carboxamido-4-quinolone agonists. TM3 was rotated by 20° anticlockwise when seen from the extracellular side. TM6 was also rotated until Cys^{257} pointed toward the pocket, resulting in a 30° anticlockwise rotation. The geometry of this final model was optimized until convergence to a 0.01 kcal/mol·Å gradient with the backbone hydrogen bonds constrained and subsequently checked to verify its structural validity. The ligands were then docked in a pocket defined as a sphere of 15 Å around Lys^{98} using the Gold software.

Using this receptor model, docking of the 3-carboxamido-4-quinolone derivatives was performed, followed by energy minimization. Nonselective CB_2 ligands, WIN-55,212-2 and CP-55,940, were used as template molecules, using the information obtained in mutants receptors to delineate the binding site. The resulting receptor-based alignments of WIN-55,212-2, CP-55,940, and **30** are illustrated in Figure 1. These results suggested that the 4-oxo-1,4-dihydroquinoline derivatives interact in the same region of the CB_2 receptor as WIN-55,212-2 and CP-55,940. However, the CB_2 cannabinoid receptor residues involved in the interactions with the ligands slightly differ between WIN-55,212-2 and CP-55,940 and derivative **30**.

Compound **30** was also docked in the cannabinoid CB_2 cannabinoid receptor active site, as shown in Figure 2. Aromatic residues are abundant in the region encompassed by transmembrane regions 3 to 5 (TM 3−TM 5), particularly near the extracellular side of the cannabinoid receptor. The hydrophobic *N*(1) alkyl side chain is perfectly positioned to interact with hydrophobic residues Ile^{110}, Cys^{175}, Pro^{178}, and Leu^{182}. The amide oxygen atom in **30** forms a hydrogen bond with Ser^{193}. The quinolone nucleus is in interaction with aromatic or hydrophobic residues Pro^{168}, Thr^{173}, Leu^{182}, Leu^{196}, and Phe^{200}. The 1-(3,5-dimethyl)adamantyl carboxamido substituent fits well in a pocket formed by various lipophilic or aromatic residues Phe^{183}, Pro^{184}, Pro^{187}, Phe^{197}, and Leu^{269}.

Conclusion

In light of these results, this series of 4-oxo-1,4-dihydroquinoline-3-carboxamide derivatives represents a new class of heterocyclic derivatives, acting as potent CB_2-selective receptor ligands. The [^{35}S]-GTPγS binding data revealed the CB_2 cannabinoid receptor agonistic properties of these derivatives. Best affinity values were obtained with compounds **28**−**30**, bearing an adamantyl-carboxamido substituent. Compounds containing aromatic moieties on the amide resulted in a decreased, albeit notable, affinity for the *h*CB_2 cannabinoid receptors, as shown by **15**, **22**, and **27**. The introduction of a steric constraint induced a marked improvement in affinity. Moreover, interactions of **32*R***, **33*R***, and **34*R*** with the CB_2 cannabinoid receptor are highly stereoselective. Whatever the carboxamido substitutent, the preferred N_1 side chain was the *n*-pentyl one. Finally, molecular modeling of **30** obtained either by superim-

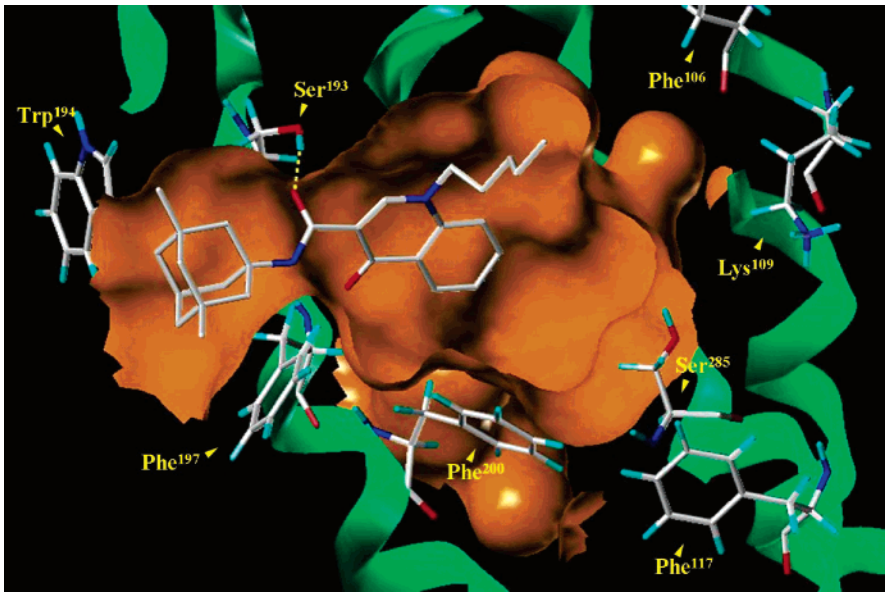

Figure 2. Compound **30** docked in the putative active site of the CB_2 receptor. Hydrogen bond is colored in yellow.

position or by docking indicated that these derivatives may share to some extent the binding mode of WIN-55,212-2.

Experimental Section

Chemistry. All commercial reagents and solvents were used without further purification. Analytical thin-layer chromatography was performed on precoated Kieselgel 60F_{254} plates (Merck); the spots were located by UV (254 and 366 nm) and/or with iodine; Rf values are given for guidance. Silica gel 60 230−400 mesh purchased from Merck was used for column chromatography. Preparative thick-layer chromatography was performed using silica gel from Merck, and the compounds were extracted from silica gel by the following solvent system: CH_2Cl_2/MeOH 70:30. All melting points were determinated with a Büchi 535 capillary appartus and remain uncorrected. ^{1}H NMR spectra were obtained using a Brücker 300 MHz spectrometer, chemical shifts (δ) were expressed in ppm relative to tetramethylsilane used as an internal standard, *J* values are in hertz, and the splitting patterns were designated as follows: s, singlet; d, doublet; t, triplet; m, multiplet. IR spectra were determined with a Brücker Vector 22 spectrometer on a germanium crystal. APCI$^+$ (atmospheric pressure chemical ionization) mass spectra were obtained on an LC-MS system Thermo Electron Surveyor MSQ. Optical rotations ($[\alpha]_D$) were measured on a Perkin-Elmer 343 polarimeter. Specific rotations are given as deg/dm; the concentration values are reported as g/mL of the specified solvent and were recorded at 25 °C. Elemental analyses were performed by the "Service Central d'Analyses" at the CNRS, Vernaison (France).

2-Phenylaminomethylene-malonic Acid Diethyl Ester (1). A mixture of 2-ethoxymethylene-malonic acid diethyl ester (9.30 mL, 46 mmol) and aniline (4.20 mL, 46 mmol) was heated at 100 °C for 4 h. Petroleum ether (100 mL) was added, and the resulting solution was cooled in an ice bath. The resulting precipitate was collected by filtration, washed with petroleum ether, and recrystallized from petroleum ether to provide 11.02 g (91%) of compound **1** as a white solid: mp 54−55 °C; IR; ^{1}H NMR ($CDCl_3$).

4-Oxo-1,4-dihydro-quinoline-3-carboxylic Acid Ethyl Ester (2). Phenyl ether (40 mL) was heated under stirring at 240 °C. The malonic acid diethyl ester (**1**) (9.50 g, 36 mmol) was slowly added, and the resulting mixture was refluxed for 4 h. After the mixture was cooled at room temperature, the resulting precipitate was collected by filtration, washed with petroleum ether, and recrystallized from DMF to provide 6.02 g (77%) of compound **2** as a white solid: mp >250 °C; IR; ^{1}H NMR (DMSO-d_6).

General Procedure for the Preparation of 1-Alkyl-4-oxo-1,4-dihydro-quinoline-3-carboxylic Acid Ethyl Ester (3−6). NaH 60% (0.22 g, 5.52 mmol) was added to a mixture of quinoline carboxilic acid ethyl ester **2** (1.00 g, 4.60 mmol) and anhydrous DMF (30 mL) under stirring at room temperature. The appropriate alkyl bromide (5.52 mmol) was added, and the mixture was stirred at 90 °C for 3 h (**3−4**) and 6 h (**5−6**). The solvent was removed under reduced pressure, and the residue subsequently dissolved in ethyl acetate. The precipitate was eliminated by filtration, and the organic layer was concentrated under reduced pressure and finally purified by flash chromatography, using dichloromethane/ethyl acetate 5:5 as eluent.

1-Butyl-4-oxo-1,4-dihydro-quinoline-3-carboxylic Acid Ethyl Ester (3). Orange oil (0.72 g, 57%); IR; ^{1}H NMR ($CDCl_3$).

4-Oxo-1-pentyl-1,4-dihydro-quinoline-3-carboxylic Acid Ethyl Ester (4). Orange oil (1.23 g, 93%); IR; ^{1}H NMR ($CDCl_3$).

1-Hexyl-4-oxo-1,4-dihydro-quinoline-3-carboxylic Acid Ethyl Ester (5). Orange oil (0.69 g, 50%); IR; ^{1}H NMR ($CDCl_3$).

1-Benzyl-4-oxo-1,4-dihydro-quinoline-3-carboxylic Acid Ethyl Ester (6). Beige solid (1.06 g, 75%); mp 120−121 °C; IR; ^{1}H NMR (DMSO-d_6).

General Procedure for the Preparation of 1-Alkyl-4-oxo-1,4-dihydro-quinoline-3-carboxylic Acid (7−10). The appropriate quinoline-3-carboxylic acid ethyl ester **3−6** (4.13 mmol) was refluxed for 3 h in a mixture of aqueous 10% sodium hydroxyde (5 mL) and ethyl alcohol (5 mL). After cooling, the solution was adjusted to pH 4 with aqueous 10% hydrochloric acid. The resulting precipitate was collected by filtration, washed with H_2O, and recrystallized from diisopropyl ether.

1-Butyl-4-oxo-1,4-dihydro-quinoline-3-carboxylic Acid (7). White solid (0.71 g, 70%); mp 165−166 °C; IR; ^{1}H NMR (DMSO-d_6).

4-Oxo-1-pentyl-1,4-dihydro-quinoline-3-carboxylic Acid (8). White solid (0.81 g, 76%); mp 135−137 °C; IR; ^{1}H NMR (DMSO-d_6).

1-Hexyl-4-oxo-1,4-dihydro-quinoline-3-carboxylic Acid (9). White solid (0.67 g, 75%); mp 150−151 °C; IR; ^{1}H NMR (DMSO-d_6).

1-Benzyl-4-oxo-1,4-dihydro-quinoline-3-carboxylic Acid (10). White solid (0.86 g, 75%); mp 175−176 °C; IR; ^{1}H NMR (DMSO-d_6).

General Procedure for the Preparation of *N*3-aryl-1-alkyl-4-oxo-1,4-dihydroquinoline-3-carboxamide (11−36). To a solution of PybrOP (1.5 mmol) in 3 mL of dry DMF were added at room temperature compounds **7-10** and diisopropylethylamine (3.0 mmol). The preswollen resin (0.75 g) in dry DMF was treated with the above mixture at room temperature for 3 h, after which time the resin was washed three times with dry DMF and three times with dichloromethane. The same activation procedure was repeated a second time. The appropriate amine (0.67 mmol) dissolved in dry DMF was reacted with the polymer-bound activated ester for 24 h at room temperature. The supernatant was then separated from the resin by filtration and the polymer beads washed three times with dry DMF and three times with dichloromethane. The combined solutions were concentrated and, the residue was purified either by crystallization or preparative TLC.

***N*3-(4-Methoxyphenyl)-1-butyl-4-oxo-1,4-dihydroquinoline-3-carboxamide (11).** Recrystallization from diisopropyl ether, yellow solid (57 mg, 24%); mp 129−130 °C; IR; ^{1}H NMR ($CDCl_3$); LC-MS (APCI$^+$) *m/z* 351 (MH^+). Anal. ($C_{21}H_{22}N_2O_3$) C, H, N.

***N*3-(4-Methoxyphenyl)-4-oxo-1-pentyl-1,4-dihydroquinoline-3-carboxamide (12).** Recrystallization from diisopropyl ether, yellow solid (34 mg, 14%); mp 134−135 °C; IR; ^{1}H NMR ($CDCl_3$); LC-MS (APCI$^+$) *m/z* 365 (MH^+). Anal. ($C_{22}H_{24}N_2O_3$) C, H, N.

***N*3-(4-Methoxyphenyl)-1-hexyl-4-oxo-1,4-dihydroquinoline-3-carboxamide (13).** Recrystallization from diisopropyl ether, yellow solid (130 mg, 51%); mp 119−120 °C; IR; ^{1}H NMR ($CDCl_3$); LC-MS (APCI$^+$) *m/z* 379 (MH^+). Anal. ($C_{23}H_{26}N_2O_3$) C, H, N.

***N*3-(1-Naphthyl)-1-butyl-4-oxo-1,4-dihydroquinoline-3-carboxamide (14).** Recrystallization from ethyl acetate, white solid (90 mg, 36%); mp 174−175 °C; IR; ^{1}H NMR ($CDCl_3$); LC-MS (APCI$^+$) *m/z* 371 (MH^+). Anal. ($C_{24}H_{22}N_2O_2$) C, H, N.

***N*3-(1-Naphthyl)-4-oxo-1-pentyl-1,4-dihydroquinoline-3-carboxamide (15).** Recrystallization from ethyl acetate, white solid (184 mg, 71%); mp 184−185 °C; IR; ^{1}H NMR ($CDCl_3$); LC-MS (APCI$^+$) *m/z* 385 (MH^+). Anal. ($C_{25}H_{24}N_2O_2$) C, H, N.

***N*3-(1-Naphthyl)-1-hexyl-4-oxo-1,4-dihydroquinoline-3-carboxamide (16).** Recrystallization from ethyl acetate, white solid (81 mg, 30%); mp 158−159 °C; IR; ^{1}H NMR ($CDCl_3$); LC-MS (APCI$^+$) *m/z* 399 (MH^+). Anal. ($C_{26}H_{26}N_2O_2$) C, H, N.

***N*3-(Benzyl)-1-butyl-4-oxo-1,4-dihydroquinoline-3-carboxamide (17).** Recrystallization from *n*-heptane, white solid (70 mg, 31%); mp 165−166 °C; IR; ^{1}H NMR ($CDCl_3$); LC-MS (APCI$^+$) *m/z* 335 (MH^+). Anal. ($C_{21}H_{22}N_2O_2$) C, H, N.

***N*3-(Benzyl)-4-oxo-1-pentyl-1,4-dihydroquinoline-3-carboxamide (18).** Recrystallization from *n*-heptane, white solid (143 mg, 61%); mp 170−171 °C; IR; ^{1}H NMR ($CDCl_3$); LC-MS (APCI$^+$) *m/z* 349 (MH^+). Anal. ($C_{22}H_{24}N_2O_2$) C, H, N.

***N*3-(Benzyl)-1-hexyl-4-oxo-1,4-dihydroquinoline-3-carboxamide (19).** Recrystallization from *n*-heptane, white solid (102 mg, 42%); mp 176−177 °C; IR; ^{1}H NMR ($CDCl_3$); LC-MS (APCI$^+$) *m/z* 363 (MH^+). Anal. ($C_{23}H_{26}N_2O_2$) C, H, N.

***N*3-(4-Methoxybenzyl)-4-oxo-1-pentyl-1,4-dihydroquinoline-3-carboxamide (20).** Purified by TLC eluting from cyclohexane/ethyle acetate 6:4, yellow oil (140 mg, 55%); IR; LC-MS (APCI$^+$) *m/z* 379 (MH^+). Anal. ($C_{23}H_{26}N_2O_3$) C, H, N.

***N*3-(2-Naphthyl)-4-oxo-1-pentyl-1,4-dihydroquinoline-3-carboxamide (21).** Recrystallization from ethyl acetate, white solid (129 mg, 50%); mp 162−163 °C; IR; ^{1}H NMR ($CDCl_3$); LC-MS ($APCI^+$) *m/z* 385 (MH^+). Anal. ($C_{25}H_{24}N_2O_2$) C, H, N.

***N*3-(Phenethyl)-4-oxo-1-pentyl-1,4-dihydroquinoline-3-carboxamide (22).** Purified by TLC eluting from cyclohexane/ethyle acetate 6:4, yellow oil (188 mg, 77%); IR; ^{1}H NMR ($CDCl_3$); LC-MS ($APCI^+$) *m/z* 363 (MH^+). Anal. ($C_{23}H_{26}N_2O_2$) C, H, N.

***N*3-(3-Phenylpropyl)-4-oxo-1-pentyl-1,4-dihydroquinoline-3-carboxamide (23).** Purified by TLC eluting from dichloromethane/methyl alcohol 95:5, white solid (162 mg, 64%); mp 78−79 °C; IR; ^{1}H NMR ($CDCl_3$); LC-MS ($APCI^+$) *m/z* 377 (MH^+). Anal. ($C_{24}H_{28}N_2O_2$) C, H, N.

***N*3-(3,4-Dichlorophenyl)-4-oxo-1-pentyl-1,4-dihydroquinoline-3-carboxamide (24).** Purified by TLC eluting from cyclohexane/ethyl acetate 6:4, white solid (201 mg, 74%); mp 175−176 °C; IR; ^{1}H NMR ($CDCl_3$); LC-MS ($APCI^+$) *m/z* 404 (MH^+). Anal. ($C_{21}H_{20}N_2O_2Cl_2$) C, H, N.

***N*3-(4-Cyanophenyl)-4-oxo-1-pentyl-1,4-dihydroquinoline-3-carboxamide (25).** Purified by TLC eluting from cyclohexane/ethyl acetate 6:4, white solid (111 mg, 46%); mp 119−120°C; IR; ^{1}H NMR ($CDCl_3$); LC-MS ($APCI^+$) *m/z* 360 (MH^+). Anal. ($C_{22}H_{21}N_3O_2$) C, H, N.

***N*3-(4-Biphenyl)-4-oxo-1-pentyl-1,4-dihydroquinoline-3-carboxamide (26).** Purified by TLC eluting from cyclohexane/ethyl acetate 6:4, white solid (108 mg, 39%); mp 153−154°C; IR; ^{1}H NMR ($CDCl_3$); LC-MS ($APCI^+$) *m/z* 411 (MH^+). Anal. ($C_{27}H_{26}N_2O_2$) C, H, N.

***N*3-(2-(Benzo[1,3]dioxol-5-yl)ethyl)-4-oxo-1-pentyl-1,4-dihydroquinoline-3-carboxamide (27).** Purified by TLC eluting from dichloromethane/methyl alcohol 95:5, white solid (121 mg, 44%); mp 85−86°C; IR; ^{1}H NMR ($CDCl_3$); LC-MS ($APCI^+$) *m/z* 407 (MH^+). Anal. ($C_{24}H_{26}N_2O_4$) C, H, N.

***N*3-(1-Adamantyl)-4-oxo-1-pentyl-1,4-dihydroquinoline-3-carboxamide (28).** Recrystallization from *n*-heptane, white solid (144 mg, 55%); mp 184−185 °C; IR; ^{1}H NMR ($CDCl_3$); LC-MS ($APCI^+$) *m/z* 393 (MH^+). Anal. ($C_{25}H_{32}N_2O_2$) C, H, N.

***N*3-(2-Adamantyl)-4-oxo-1-pentyl-1,4-dihydroquinoline-3-carboxamide (29).** Recrystallization from *n*-heptane, white solid (118 mg, 45%); mp 180−181 °C; IR; ^{1}H NMR ($CDCl_3$); LC-MS ($APCI^+$) *m/z* 393 (MH^+). Anal. ($C_{25}H_{32}N_2O_2$) C, H, N.

***N*3-(1-(3,5-Dimethyl)adamantyl)-4-oxo-1-pentyl-1,4-dihydroquinoline-3-carboxamide (30).** Recrystallization from *n*-heptane, white solid (190 mg, 67%); mp 164−165 °C; IR; ^{1}H NMR ($CDCl_3$); LC-MS ($APCI^+$) *m/z* 421 (MH^+). Anal. ($C_{27}H_{36}N_2O_2$) C, H, N.

***N*3-(1-(3,5-Dimethyl)adamantyl)-4-oxo-1-benzyl-1,4-dihydroquinoline-3-carboxamide (31).** Recrystallization from *n*-heptane, white solid (221 mg, 70%); mp 174−175 °C; IR; ^{1}H NMR ($CDCl_3$); LC-MS ($APCI^+$) *m/z* 441 (MH^+). Anal. ($C_{29}H_{32}N_2O_2$) C, H, N.

***(RS)-N*3-(1-Phenylethyl)-4-oxo-1-pentyl-1,4-dihydroquinoline-3-carboxamide (32).** Purified by TLC eluting from cyclohexane/ethyl acetate 6:4, white oil (188 mg, 77%); $[\alpha]_D^{25} = 0°$, $c = 0.01$, CH_2Cl_2; IR; ^{1}H NMR ($CDCl_3$); LC-MS ($APCI^+$) *m/z* 363 (MH^+). Anal. ($C_{23}H_{26}N_2O_2$) C, H, N.

***(R)-N*3-(1-Phenylethyl)-4-oxo-1-pentyl-1,4-dihydroquinoline-3-carboxamide (32*R*).** Purified by TLC eluting from cyclohexane/ethyl acetate 6:4, white oil (237 mg, 97%); $[\alpha]_D^{25} = -95°$, $c = 0.01$, CH_2Cl_2; IR; ^{1}H NMR ($CDCl_3$); LC-MS ($APCI^+$) *m/z* 363 (MH^+). Anal. ($C_{23}H_{26}N_2O_2$) C, H, N.

***(S)-N*3-(1-Phenylethyl)-4-oxo-1-pentyl-1,4-dihydroquinoline-3-carboxamide (32*S*).** Purified by TLC eluting from cyclohexane/ethyl acetate 6:4, white oil (234 mg, 96%); $[\alpha]_D^{25} = +95°$, $c = 0.01$, CH_2Cl_2; IR; ^{1}H NMR ($CDCl_3$); LC-MS ($APCI^+$) *m/z* 363 (MH^+). Anal. ($C_{23}H_{26}N_2O_2$) C, H, N.

(*RS*)-*N*3-(1-(2-Naphthyl)ethyl)-4-oxo-1-pentyl-1,4-dihydroquinoline-3-carboxamide (33). Purified by TLC eluting from cyclohexane/ethyl acetate 6:4, white oil (220 mg, 79%); $[\alpha]_D^{25} = 0°$, $c = 0.01$, CH_2Cl_2; IR; ^{1}H NMR ($CDCl_3$); LC-MS ($APCI^+$) *m/z* 413 (MH^+). Anal. ($C_{27}H_{28}N_2O_2$) C, H, N.

***(R)-N*3-(1-(2-Naphthyl)ethyl)-4-oxo-1-pentyl-1,4-dihydroquinoline-3-carboxamide (33*R*).** Purified by TLC eluting from cyclohexane/ethyl acetate 6:4, white oil (203 mg, 73%); $[\alpha]_D^{25} = -151°$, $c = 0.01$, CH_2Cl_2; IR; ^{1}H NMR ($CDCl_3$); LC-MS ($APCI^+$) *m/z* 413 (MH^+). Anal. ($C_{27}H_{28}N_2O_2$) C, H, N.

***(S)-N*3-(1-(2-Naphthyl)ethyl)-4-oxo-1-pentyl-1,4-dihydroquinoline-3-carboxamide (33*S*).** Purified by TLC eluting from cyclohexane/ethyl acetate 6:4, white oil (239 mg, 86%); $[\alpha]_D^{25} = +151°$, $c = 0.01$, CH_2Cl_2; IR; ^{1}H NMR ($CDCl_3$); LC-MS ($APCI^+$) *m/z* 413 (MH^+). Anal. ($C_{27}H_{28}N_2O_2$) C, H, N.

***(RS)-N*3-(1-(1-Naphthyl)ethyl)-4-oxo-1-pentyl-1,4-dihydroquinoline-3-carboxamide (34).** Purified by TLC eluting from cyclohexane/ethyl acetate 6:4, white oil (150 mg, 54%); $[\alpha]_D^{25} = 0°$, $c = 0.01$, CH_2Cl_2; IR; ^{1}H NMR ($CDCl_3$); LC-MS ($APCI^+$) *m/z* 413 (MH^+). Anal. ($C_{27}H_{28}N_2O_2$) C, H, N.

***(R)-N*3-(1-(1-Naphthyl)ethyl)-4-oxo-1-pentyl-1,4-dihydroquinoline-3-carboxamide (34*R*).** Purified by TLC eluting from cyclohexane/ethyl acetate 6:4, white oil (228 mg, 82%); $[\alpha]_D^{25} = -200°$, $c = 0.01$, CH_2Cl_2; IR; ^{1}H NMR ($CDCl_3$); LC-MS ($APCI^+$) *m/z* 413 (MH^+). Anal. ($C_{27}H_{28}N_2O_2$) C, H, N.

***(S)-N*3-(1-(1-Naphthyl)ethyl)-4-oxo-1-pentyl-1,4-dihydroquinoline-3-carboxamide (34*S*).** Purified by TLC eluting from cyclohexane/ethyl acetate 6:4, white oil (217 mg, 78%); $[\alpha]_D^{25} = +200°$, $c = 0.01$, CH_2Cl_2; IR; ^{1}H NMR ($CDCl_3$); LC-MS ($APCI^+$) *m/z* 413 (MH^+). Anal. ($C_{27}H_{28}N_2O_2$) C, H, N.

***(RS)-N*3-(1-(1,2,3,4-Tetrahydronaphthyl))-4-oxo-1-pentyl-1,4-dihydroquinoline-3-carboxamide (35).** Purified by TLC eluting from cyclohexane/ethyl acetate 7:3, white oil (143 mg, 55%); $[\alpha]_D^{25} = 0°$, $c = 0.01$, CH_2Cl_2; IR; ^{1}H NMR ($CDCl_3$); LC-MS ($APCI^+$) *m/z* 389 (MH^+). Anal. ($C_{25}H_{28}N_2O_2$) C, H, N.

3-(Morpholino-4-carbonyl)-1-pentyl-1,4-dihydroquinolin-4-one (36). Purified by TLC eluting from *n*-heptane/ethyl acetate 6:4, white oil (177 mg, 80%); IR; ^{1}H NMR (DMSO-d_6); LC-MS ($APCI^+$) *m/z* 329 (MH^+). Anal. ($C_{25}H_{32}N_2O_2$) C, H, N.

Pharmacology. Fatty acid free bovine serum albumin (BSA) was purchased from Sigma Chemical Co (St. Louis, MO). WIN-55,21-2 was purchased from RBI (Natick, MA), HU-210 and CP-55,940 were acquired from Tocris (Bristol, U.K.). SR-141716A and SR-144528 were kindly donated by Sanofi Recherche (Montpellier, France).

Cell Culture and Preparation of *h*CB_1- or *h*CB_2-Transfected CHO Cell Membranes. CHO cells stably transfected with the cDNA sequences encoding either the human CB_1 or the human CB_2 cannabinoid receptors were kindly donated by Dr. M. Detheux and Dr. P. Nokin, respectively (Euroscreen s.a., Gosselies, Belgium). Cells were grown in Ham's F12 nutrient mixture supplemented with 10% FBS, 2.5 μL/mL fungizone, 100 U/mL penicillin, 100 μg/mL streptomycin, and 400 μg/mL G418. Once at confluence, the cells were trypsinized and collected by centrifugation at 100*g* for 10 min. The following steps were performed on ice. The pellet was lysed in ice-cold 50 mM Tris-HCl, pH 7.4, and the homogenate was centrifuged at 15 000*g* for 10 min. The resulting pellet (membranes) was washed twice with the same solution under identical conditions. The protein content was determined as described by Bradford[52] using Coomasie Blue (Biorad, Belgium) with bovine serum albumin as standard.

Competition Binding Assay. [^{3}H]-SR-141716A (52 Ci/mol) was purchased from Amersham (Roosendaal, The Netherlands) and [^{3}H]-CP-55,940 (101 Ci/mol) from NEN Life Science (Zaventem, Belgium). Glass fiber filters were purchased from Whatman (Maidstone, U.K.), while Aqualuma was from PerkinElmer (Schaesberg, The Netherlands). Stock solutions of the compounds were prepared in DMSO and further diluted (100×) with the binding buffer to the desired concentration. Final DMSO concentrations in the assay were less than 0.1%.

Under these conditions, using [^{3}H]-SR-141716A, the B_{max} value was 57 pmol/mg protein and the K_d value was 1.13 (0.13 nM) for the *h*CB_1 cannabinoid receptor. Using [^{3}H]-CP-55,940, the B_{max} value was 57 pmol/mg protein and the K_d value was 4.3 (0.13 nM) for the *h*CB_2 cannabinoid receptor.

The competitive binding experiments were performed using [^{3}H]-SR-141716A (1 nM) or [^{3}H]-CP-55,940 (1 nM) as radioligands for the *h*CB_1 and the *h*CB_2 cannabinoid receptor, respectively, at

30 °C in plastic tubes, and 40 μg of membranes per tube resuspended in 0.5 mL (final volume) of binding buffer (50 mM Tris-HCl, 3 mM $MgCl_2$, 1 mM EDTA, 0.5% bovine serum albumine, pH 7.4). The test compounds were present at varying concentrations, and the nonspecific binding was determined in the presence of 10 μM HU-210. After 1 h the incubation was stopped, and the solutions were rapidly filtered through 0.5% PEI pretreated GF/B glass fiber filters on a M-48T Brandell cell harvester and washed twice with 5 mL ice-cold binding buffer without serum albumin. The radioactivity on the filters was measured in a Pharmacia Wallac 1410 β-counter using 10 mL of Aqualuma, after 10 s shaking and 3 h resting. Assays were performed at least in triplicate.

[^{35}S]-GTPγS Assays. [^{35}S]-GTPγS (1173 Ci/mmol) was purchased from Amersham (Roosendaal, The Netherlands). The binding experiments were performed at 30 °C in plastic tubes containing 40 μg of protein in 0.5 mL (final volume) of binding buffer (50 mM Tris-HCl, 3 mM $MgCl_2$, 1 mM EDTA, 100 mM NaCl, 0.1% bovine serum albumin, pH 7.4) supplemented with 20 μM GDP. The test compounds were present at varying concentrations, and the nonspecific binding was measured in the presence of 100 μM Gpp(NH)p. The assay was initiated by the addition of [^{35}S]-GTPγS (0.05 nM, final concentration). The tubes were incubated for 1 h. The incubations were terminated by the addition of 5 mL ice-cold washing buffer (50 mM Tris-HCl, 3 mM $MgCl_2$, 1 mM EDTA, 100mM NaCl). The suspension was immediately filtered through GF/B filters using a 48-well Brandell cell harvester and washed twice with the same ice-cold buffer. The radioactivity on the filters was counted as mentioned above. Assays were performed in triplicate.

Data Analysis. IC_{50} and EC_{50} values were determined by nonlinear regression analysis performed using the GraphPad prism 4.0 program (GraphPad Software, San Diego). The K_i values were calculated from the IC_{50}, based on the Cheng−Prusoff equation: $K_i = IC_{50}/(1 + L/K_d)$. Statistical significance of [^{35}S]-GTPγS assay results was assessed using a one-way ANOVA followed by a Dunett post-test.

Molecular Modeling. All the calculations have been carried out under the Sybyl 6.9 modeling software[53] running on Silicon Graphics Octane 2 workstations. The construction of a homology model of the CB_2 cannabinoid receptor was realized by aligning its sequence on the bovine rhodopsine (PIR entry 1OOBO)[54] with ClustalW[55] then transferring the 3D coordinates of the rhodopsine crystallographic structure (PDB entry 1U19)[56] with Jackal.[57] To build a model in a putative activated conformation, transmembrane domains 3 and 6 (TM3 and TM6) were rotated as described for the CB_1 cannabinoid receptor by McAllister and co-workers.[51] Three-dimensional models of WIN-55,212-2, CP-55,940, and compound **30** were built from a standard fragments library, and their geometry was subsequently optimized using the Tripos force field[58] including the electrostatic term calculated from Gasteiger and Hückel atomic charges. The method of Powell available in the Maximin2 procedure was used for energy minimization until the gradient value was smaller than 0.001 kcal/mol·Å. Flexible docking of the compounds into the receptor active site was performed using GOLD[59] software. For each compound, the most stable docking model was selected according to the best scored conformation predicted by the GoldScore[59] and X-Score[60] scoring functions. The complexes were energy-minimized using the Powell method available in the Maximin2 procedure with the Tripos force field and a dielectric constant of 4.0 until the gradient value reached 0.01 kcal/mol·Å.

Acknowledgment. G.G.M. is very indebted to "Fonds pour la formation à la Recherche dans l'Industrie et l'Agriculture (FRIA, Belgium)" for the award of a research fellowship.

Supporting Information Available: 2D ^{1}H NMR (ROESY) data of **15**, elemental analysis results of **11**−**36**, and spectroscopic data for all compounds. This material is available free of charge via the Internet at http://pubs.acs.org.

References

(1) Gaoni, Y.; Mechoulam, R. Isolation, structure and partial synthesis of an active constituent of hashish. *J. Am. Chem. Soc.* **1964**, *86*, 1646−1647.
(2) Khanolkar, D. A.; Palmer, S. L.; Makriyannis, A. Molecular probes for the cannabinoid receptors. *Chem. Phys. Lipids* **2000**, *108*, 37−52.
(3) Devane, W. A.; Dysarz, F. A.; Johnson, M. R.; Melvin, L. S.; Howlett, A. C. Determination and characterization of a cannabinoid receptor in rat brain. *Mol. Pharmacol.* **1988**, *34*, 605−613.
(4) Munro, S.; Thomas, K. L.; Abu-Shaar, M. Molecular characterization of a peripheral receptor for cannabinoids. *Nature* **1993**, *365*, 61−65.
(5) Begg, M.; Pacher, P.; Bátkai, S.; Osei-Hyiaman, D.; Offertáler, L.; Mo, F. M.; Liu, J.; Kunos, G. Evidence for novel cannabinoid receptors. *Pharmacol. Ther.* **2005**, *106*, 133−145.
(6) Howlett, A. C. Cannabinoid inhibition of adenylate cyclase: relative activity of constituents and metabolites of marihuana. *Neuropharmacology* **1987**, *26*, 507−512.
(7) Mackie, K.; Hille, B. Cannabinoids inhibit N-type calcium channels in neuroblastoma-glioma cells. *Proc. Natl. Acad. Sci. U.S.A.* **1992**, *89*, 3825−3829.
(8) Gebremedhin, D.; Lange, A. R.; Campbell, W. B.; Hillard, C. J.; Harder, D. R. Cannabinoid CB_1 receptor of cat cerebral arterial muscle functions to inhibit L-type Ca^{2+} channel current. *Am. J. Physiol.* **1999**, *276*, H2085−2093.
(9) Deadwyler, S. A.; Hampson, R. E.; Mu, J.; Whyte, A.; Childers, S. Cannabinoids modulate voltage sensitive potassium A-current in hippocampal neurons via a cAMP-dependent process. *J. Pharmacol. Exp. Ther.* **1995**, *273*, 734−743.
(10) Bouaboula, M.; Poinot-Chazel, C.; Bourrie, B.; Canat, X.; Calandra, B.; Rinaldi-Carmona, M.; Le Fur, G.; Casellas, P. Activation of mitogen-activated protein kinases by stimulation of the central cannabinoid receptor CB_1. *Biochem. J.* **1995**, *312*, 637−641.
(11) Muccioli, G. G.; Lambert, D. M. Current knowledge on the antagonists and inverse agonists of cannabinoid receptors. *Curr. Med. Chem.* **2005**, *12*, 1361−1394.
(12) Lambert, D. M.; Fowler, C. J. The endocannabinoid system: drug targets, lead compounds and potential therapeutic applications. *J. Med. Chem.* **2005**, *48*, 5059−5087.
(13) Ibrahim, M. M.; Porreca, F.; Lai, J.; Albrecht, P. J.; Rice, F. L.; Khodorova, A.; Davar, G.; Makriyannis, A.; Vanderah, T. W.; Mata, H. P.; Malan, T. P. Jr. CB_2 cannabinoid receptor activation produces antinociception by stimulating peripheral release of endogenous opioids. *Proc. Natl. Acad. Sci. U S A.* **2005**, *102*, 3093−3098.
(14) Elmes, S. J.; Jhaveri, M. D.; Smart, D.; Kendall, D. A.; Chapman, V. Cannabinoid CB_2 receptor activation inhibits mechanically evoked responses of wide dynamic range dorsal horn neurons in naive rats and in rat models of inflammatory and neuropathic pain. *Eur. J. Neurosci.* **2004**, *20*, 2311−2320.
(15) Oka, S.; Yanagimoto, S.; Ikeda, S.; Gokoh, M.; Kishimoto, S.; Waku, K.; Ishima, Y.; Sugiura, T. Evidence for the involvement of the cannabinoid CB_2 receptor and its endogenous ligand 2-arachidonoylglycerol in 12-*O*-tetradecanoylphorbol-13-acetate-induced acute inflammation in mouse ear. *J. Biol. Chem.* **2005**, *280*, 18488−18497.
(16) Sarfaraz, S.; Afaq, F.; Adhami, V. M.; Mukhtar, H. Cannabinoid receptor as a novel target for the treatment of prostate cancer. *Cancer Res.* **2005**, *65*, 1635−1641.
(17) Julien, B.; Grenard, P.; Teixeira-Clerc, F.; Van Nhieu, J. T.; Li, L.; Karsak, M.; Zimmer, A. Mallat, A.; Lotersztajn, S. Antifibrogenic role of the cannabinoid receptor CB_2 in the liver. *Gastroenterology* **2005**, *128*, 742−755.
(18) Franklin, A.; Stella, N. Arachidonylcyclopropylamide increases microglial cell migration through cannabinoid CB_2 and abnormal-cannabidiol-sensitive receptors. *Eur. J. Pharmacol.* **2003**, *474*, 195−198.
(19) Stella, N. Cannabinoid signaling in glial cells. *Glia* **2004**, *48*, 267−277.
(20) Ramirez, B. G.; Blazquez, C.; Gomez del Pulgar, T.; Guzman, M.; de Ceballos, M. L. Prevention of Alzheimer's disease pathology by cannabinoids: neuroprotection mediated by blockade of microglial activation. *J. Neurosci.* **2005**, *25*, 1904−1913.
(21) Harrison, C.; Traynor, J. R. The [^{35}S]GTPgammaS binding assay: approaches and applications in pharmacology. *Life Sci.* **2003**, *74*, 489−508.
(22) Di Marzo, V.; Bisogno, T.; De Petrocellis, L.; Melck, D.; Martin, B. R. Cannabimimetic fatty acid derivatives: the anandamide family and other endocannabinoids. *Curr. Med. Chem.* **1999**, *6*, 721−744.

(23) Jagerovic, N.; Hernandez-Folgado, L.; Alkorta, I.; Goya, P.; Navarro, M.; Serrano, A.; Rodriguez de Fonseca, F.; Dannert, M. T.; Alsasua, A.; Suardiaz, M.; Pascual, D.; Martin, M. I. Discovery of 5-(4-chlorophenyl)-1-(2,4-dichlorophenyl)-3-hexyl-1*H*-1,2,4-triazole, a novel in vivo cannabinoid antagonist containing a 1,2,4-triazole motif. *J. Med. Chem.* **2004**, *47*, 2939−2942.

(24) Lange, J. H. M.; Van Stuivenberg, H. H.; Coolen, H. K. A. C.; Adolfs, T. J. P.; McCreary, A. C.; Keizer, H. G.; Wals, H. C.; Veerman, W.; Borst, A. J. M.; De Looff, W.; Verveer, P. C.; Kruse, C. G. Bioisosteric replacements of the pyrazole moiety of rimonabant: synthesis, biological properties, and molecular modeling investigations of thiazoles, triazoles, and imidazoles as potent and selective CB_1 cannabinoid receptor antagonists. *J. Med. Chem.* **2005**, *48*, 1823−1838.

(25) Plummer, C. W.; Finke, P. E.; Mills, S. G.; Wang, J.; Tong, X.; Doss, G. A.; Fong, T. M.; Lao, J. Z.; Schaeffer, M.-T.; Chen, J.; Shen, C.-P.; Stribling, D. S.; Shearman, L. P.; Starck, A. M.; Van der Ploeg, L. H. T. Synthesis and activity of 4,5-diarylimidazoles as human CB_1 receptor inverse agonists. *Bioorg. Med. Chem. Lett.* **2005**, *15*, 1441−1446.

(26) Ooms, F.; Wouters, J.; Oscari, O.; Happaerts, T.; Bouchard, G.; Carrupt, P.-A.; Testa, B.; Lambert, D. M. Exploration of the pharmacophore of 3-alkyl-5-arylimidazolidinediones as new CB_1 cannabinoid receptor ligands and potential antagonists: synthesis, lipophilicity, affinity and molecular modeling. *J. Med. Chem.* **2002**, *45*, 1748−1756.

(27) Muccioli, G. G.; Martin, D.; Scriba, G. K.; Poppitz, W.; Poupaert, J. H.; Wouters, J.; Lambert, D. M. Substituted 5,5′-diphenyl-2-thioxoimidazolidin-4-one as CB_1 cannabinoid receptor ligands: synthesis and pharmacological evaluation. *J. Med. Chem.* **2005**, *48*, 2509−2517.

(28) Meurer, L. C.; Finke, P. E.; Mills, S. G.; Walsh, T. F.; Toupence, R. B.; Goulet, M. T.; Wang, J.; Tong, X.; Fong, T. M.; Lao, J.; Schaeffer, M.-T.; Chen, J.; Shen, C.-P.; Stribling, D. S.; Shearman, L. P.; Starck, A. M.; Van der Ploeg, L. H. T. Synthesis and SAR of 5,6-diarylpyridines as human CB_1 inverse agonists. *Bioorg. Med. Chem. Lett.* **2005**, *15*, 645−651.

(29) Iwamura, H.; Suzuki, H.; Ueda, Y.; Kaya, T.; Inaba, T. In vitro and in vivo pharmacological characterization of JTE-907, a novel selective ligand for cannabinoid CB_2 receptor. *J. Pharmacol. Exp. Ther.* **2001**, *296*, 420−425.

(30) Ferrarini, P. L.; Calderone, V.; Cavallini, T.; Manera, C.; Saccomanni, G.; Pani, L.; Ruiu, S.; Gessa, G. L. Synthesis and biological evaluation of 1,8-naphthyridin-4(1*H*)-on-3-carboxamide derivatives as new ligands of cannabinoid receptors. *Bioorg. Med. Chem.* **2004**, *12*, 1−13.

(31) Lavey, B. J.; Kozlowski, J. A.; Hipkin, R. W.; Gonsiorek, W.; Lundell, D. J.; Piwinski, J. J.; Naruba, S.; Lunn, C. A. Triaryl bissulfones as a new class of cannabinoid CB_2 receptor inhibitors: identification of a lead and initial SAR studies. *Bioorg. Med. Chem. Lett.* **2005**, *15*, 783−786.

(32) Pertwee, R. G. Pharmacology of cannabinoid receptor ligands. *Curr. Med. Chem.* **1999**, *6*, 635−664.

(33) Buckley, N. E.; McCoy, K. L.; Mezey, E.; Bonner, T.; Zimmer, A.; Felder, C. C.; Glass, M.; Zimmer A. Immunomodulation by cannabinoids is absent in mice deficient for the cannabinoid CB_2 receptor. *Eur. J. Pharmacol.* **2000**, *396*, 141−149.

(34) Nackley, A. G.; Makriyannis, A.; Hohmann, A. G. Selective activation of cannabinoid CB_2 receptors suppresses spinal fos protein expression and pain behavior in a rat model of inflammation. *Neuroscience* **2003**, *119*, 747−757.

(35) Malan, T. P., Jr.; Ibrahim, M. M.; Deng, H.; Liu, Q.; Mata, H. P.; Vanderah, T.; Porreca, F.; Makriyannis, A. CB_2 cannabinoid receptor-mediated peripheral antinociception. *Pain* **2001**, *93*, 239−245.

(36) Malan, T. P., Jr.; Ibrahim, M. M.; Vanderah, T. W.; Makriyannis, A.; Porreca, F. Inhibition of pain responses by activation of CB_2 cannabinoid receptors. *Chem. Phys. Lipids* **2002**, *121*, 191−200.

(37) Malan, T. P., Jr.; Ibrahim, M. M.; Lai, J.; Vanderah, T. W.; Makriyannis, A.; Porreca, F. CB_2 cannabinoid receptor agonist: pain relief without psychoactive effects? *Curr. Opin. Pharmacol.* **2003**, *3*, 62−67.

(38) Steffens, S.; Veillard, N. R.; Arnaud, C.; Pelli, G.; Burger, F.; Staub, C.; Zimmer, A.; Frossard, J. L.; Mach, F. Low dose oral cannabinoid therapy reduces progression of atherosclerosis in mice. *Nature* **2005**, *434*, 708−709.

(39) Huffman, J. W.; Padgett, L. W. Recent Developments in the Medicinal Chemistry of Cannabimetic Indoles, Pyrroles and Indenes. *Curr. Med. Chem.* **2005**, *12*, 1395−1411.

(40) Kanyonyo, M. R.; Govaerts, S. J.; Hermans, E.; Poupaert, J. H.; Lambert, D. M. 3-Alkyl-(5,5′-diphenyl)imidazolidinediones as new cannabinoid receptor ligands. *Bioorg. Med. Chem. Lett.* **1999**, *9*, 2233−2236.

(41) Gould, R. G.; Jacobs, W. A. The synthesis of certain substituted quinolines and 5,6-benzoquinolines. *J. Am. Chem. Soc.* **1939**, *61*, 2890−2895.

(42) Price, C. C.; Roberts, R. M. The synthesis of 4-hydroxyquinolines. *J. Am. Chem. Soc.* **1946**, *68*, 1204−1208.

(43) Leyva, E.; Monreal, E.; Hernandez, A. Synthesis of fluoro-4-hydroxyquinoline-3-carboxylic acids by the Gould-Jacobs reaction. *J. Fluorine Chem.* **1999**, *94*, 7−10.

(44) Zhang, M. Q.; Levshin, I.; Vanden Berghe, D.; Haemers, A. Synthesis and antibacterial evolution of 1-(4-thiazolylmethyl)- and 7-(4-thiazolylmethyl)amino-substituted quinolones. *Eur. J. Med. Chem.* **1991**, *26*, 331−334.

(45) Jung, J.-C.; Jung, Y.-J.; Park, O.-S. Synthesis of 4-hydroxyquinolin-2(1*H*)-one analogues and 2-substituted quinolone derivatives. *J. Het. Chem.* **2001**, *38*, 61−67.

(46) Salmon-Chemin, L.; Lemaire, A.; De Freitas, S.; Déprez, B.; Sergheraert, C.; Davioud-Charvet, E. Parrallel synthesis of a library of 1,4-naphthoquinones and automated screening of potential inhibitors of trypanothione reductase from *Trypanosoma cruzi*. *Bioorg. Med. Chem. Lett.* **2000**, *10*, 631−635.

(47) Pop, I. E.; Déprez, B. P.; Tartar, A. L. Versatile acylation of *N*-nucleophiles using a new polymer-supported 1-hydroxybenzotriazole derivative. *J. Org. Chem.* **1997**, *62*, 2594−2603.

(48) Govaerts, S. J.; Hermans, E.; Lambert, D. M. Comparison of cannabinoid ligands affinities and efficacies in murine tissues and in transfected cells expressing human recombinant cannabinoid receptors. *Eur. J. Pharm. Sci.* **2004**, *23*, 233−243.

(49) Govaerts, S. J.; Muccioli, G. G.; Hermans, E.; Lambert, D. M. Characterization of the pharmacology of imidazolidinedione derivatives at cannabinoid CB_1 and CB_2 receptors. *Eur. J. Pharmacol.* **2004**, *495*, 43−53.

(50) Lu, D.; Meng, Z.; Thakur, G. A.; Fan, P.; Steed, J.; Tartal, C. L.; Hurst, D. P.; Reggio, P. H.; Deschamps, J. R.; Parrish, D. A.; George, C.; Järbe, T. U. C.; Lamb, R. J.; Makriyannis, A. Adamantyl cannabinoids: A novel class of cannabinergic ligands. *J. Med. Chem.* **2005**, *48*, 4576−4585.

(51) McAllister, S. D.; Rizvi, G.; Anavi-Goffer, S.; Hurst, D. P.; Barnett-Norris, J.; Lynch, D. L.; Reggio, H. P.; Abood, M. E. An aromatic microdomain at the cannabinoid CB_1 receptor constitutes an agonist/inverse agonist binding domain. *J. Med. Chem.* **2003**, *46*, 5139−5152.

(52) Bradford, M. M. A rapid and sensitive method for the quantitation of microgram quantities of protein utilizing the principle of protein-dye binding. *Anal. Biochem.* **1976**, *72*, 248−254.

(53) SYBYL 6.9.1, Tripos Associates, Inc., 1699 South Hanley Road, St. Louis, MO 63144.

(54) Nathans, J.; Hogness, D. S. Isolation, sequence analysis, and intron-exon arrangement of the gene encoding bovine rhodopsin. *Cell* **1983**, *34*, 807−814.

(55) Thompson, J. P.; Higgins, D. G.; Gibson, T. J. ClustalW: improving the sensitivity of progressive sequence alignment through sequence weighting, position-specific gap penalties and weight matrix choice. *Nucleic Acids Res.* **1994**, *22*, 4673−4680.

(56) Okada, T.; Sugihara, M.; Bondar, A. N.; Elstner, M.; Entel, P.; Buss, V. The retinal conformation and its environment in rhodopsin in light of a new 2.2 Å crystal structure. *J. Mol. Biol.* **2004**, *10*, 71−83.

(57) Petrey, D.; Xiang, Z.; Tang, C. L.; Xie, L.; Gimpelev, M.; Mitros, T.; Soto, C. S.; Goldsmith-Fischman, S.; Kernytsky, A.; Schlessinger, A.; Koh, I. Y. Y.; Alexov, E.; Honig, B. Using multiple structure alignments, fast model building, and energetic analysis in fold recognition and homology modeling. *Proteins: Struct., Func. Genet.* **2003**, *53*, 430−435.

(58) Clark, M.; Cramer, R. D., III; Van Opdenbosch, N. Validation of the General Purpose Tripos 5.2 Force Field. *J. Comput. Chem.* **1989**, *10*, 982−1012.

(59) Jones, G.; Willett, P.; Glen, R. C.; Leach, A. R.; Taylor, R. Development and validation of a genetic algorithm for flexible docking. *J. Mol. Biol.* **1997**, *267*, 727−748.

(60) Wang, R.; Lai, L.; Wang, S. Further development and validation of empirical scoring functions for structure-based binding affinity prediction. *J. Comput.-Aided Mol. Des.* **2002**, *16*, 11−26.

JM050467Q